



# Electronic, elastic and dynamic properties of the filled tetrahedral semiconductor LiMgN under pressures



H.Y. Wu <sup>a,\*</sup>, Y.H. Chen <sup>b</sup>, C.R. Deng <sup>a</sup>, X.Y. Han <sup>a</sup>, Z.J. Liu <sup>c</sup>

<sup>a</sup> School of Science, Chongqing Jiaotong University, Chongqing 400074, China

<sup>b</sup> School of Chemical Engineering and Environment, North University of China, Taiyuan 030051, China

<sup>c</sup> Department of Physics, Lanzhou City University, Lanzhou 730070, China

## ARTICLE INFO

### Article history:

Received 25 May 2015

Received in revised form

28 July 2015

Accepted 29 July 2015

Available online 30 July 2015

### Keywords:

Electronic properties

Elastic properties

Dynamic properties

High pressure

## ABSTRACT

The electronic, elastic and dynamic properties of LiMgN under pressures have been studied using the plane wave pseudopotential method based on density functional theory within the local density approximation (LDA). The calculated lattice constants, bulk modulus and band gap values of the  $\alpha$  phase LiMgN at normal conditions are in good agreement with the available experimental and theoretical results. Our GW corrected band gap values 3.190 eV ( $\Gamma$ - $\Gamma$ ) and 3.033 eV ( $\Gamma$ -X) are closer to the experimental data 3.20 eV. The variations of the band gap values, elastic constants, bulk modulus, shear modulus, Young's modulus, Poisson's ratio, elastic anisotropy, microhardness, Debye temperature and melting temperature with pressure for the  $\alpha$  phase LiMgN are presented. The calculated phonon dispersion curves and the thermal properties entropy  $S$  and heat capacity  $C_V$  have also been obtained.

© 2015 Elsevier Inc. All rights reserved.

## 1. Introduction

As one of the filled tetrahedral compounds  $A^I B^II C^V$  ( $A^I = \text{Li, Cu, Ag}$ ;  $B^II = \text{Be, Mg, Zn, Cd}$ ;  $C^V = \text{N, P, As, Sb and Bi}$ ), LiMgN is of great interest owing to its particular structural and physical properties. LiMgN is a prominent material for technological applications due to its wide band gap characteristic [1–3],  $\text{MgB}_2$ -like superconducting properties [4] and favorable hydrogen storage capability [5–8].

The crystal structure of LiMgN can be described as a cubic zincblende (ZB) structure (space group  $F\bar{4}3m$ ) with Li occupying half the available tetrahedral interstitial sites. Mg cation sits at (0, 0, 0), with N at (0.25, 0.25, 0.25) and Li at (0.5, 0.5, 0.5) ( $\alpha$  phase). It is also feasible for Li to occupy either the (0.75, 0.75, 0.75) site neighboring the Mg cation position ( $\beta$  phase) or switching with N to sit in between the Mg and N site ( $\gamma$  phase) [2].

Despite much work on the structural and electronic properties of LiMgN [1–3,9–13], the majority of these work were performed using LDA or general gradient approximation (GGA). Therefore, the band gap values were always underestimated. Moreover, there are few literatures reported in detail the elastic properties and dynamical properties of LiMgN especially under pressures [10,14,15]. However, the study of the pressure dependence of the band gaps of semiconductors is of fundamental interest in order to insight into the electronic properties of materials. It is known that the elastic properties are related to the

hardness of the materials and are also linked the anisotropy character of bonding, structural stability, sound velocities, Debye temperature and so on. The knowledge of the phonon spectrum plays an important role in determining various materials properties such as phase transition, dynamical stability, transport and thermal properties.

Therefore, the detailed study of the electronic, elastic and phonon properties of LiMgN is necessary. The aim of this paper is to investigate the effect of pressure on the electronic, elastic and dynamical properties of the filled tetrahedral semiconductor LiMgN based on the density functional theory within GW correction and a linear response technique.

## 2. Theoretical methods

In our calculations, the exchange-correlation potential is adopted by LDA of Ceperly and Adler [16], parameterized by Perdew and Zunger [17] scheme. The norm-conserving pseudopotential [18] within the scheme suggested by Troullier and Martins [19] are employed to describe the electron–ion interactions. The special points sampling integration over the Brillouin zone is employed using the Monkhorst-Pack method [20] with a shifted  $8 \times 8 \times 8$   $k$ -point mesh. Well converged results are obtained using the plane-wave basis set cut-off is set as 50 Hartree. These parameters ensure the tolerance on the maximal force is  $1.0 \times 10^{-6}$  Hartree/Bohr when the geometry optimization is performed. Self-energy corrections to the density functional theory (DFT) Kohn–Sham eigenvalues are used in the GW approximation.

\* Corresponding author.

E-mail address: [hywu09@163.com](mailto:hywu09@163.com) (H.Y. Wu).

In the GW quasi-particle energy calculation, the self-energy is a convolution of the single particle Green's function  $G$  and the dynamically screened Coulomb potential. The dielectric matrix is calculated with the plasmon-pole model [21] and is used to calculate the screening. On this basis, the self-energy  $\Sigma$  matrix element at the given  $k$ -point is computed, and the GW eigenvalues for the target states at this  $k$ -point are derived. For both the screening and the self-energy calculation, 100 bands are chosen to ensure the convergence of the GW band gap. Having obtained self-consistent solutions of the Kohn–Sham equation, phonon dispersion spectra is constructed using density functional perturbation theory (DFPT) in the linear response approach [22,23], in which second order derivatives of the total energy are calculated to obtain a dynamical matrix, which avoids the use of supercells and allows the calculation of the dynamical matrix at arbitrary  $q$  vectors.  $4 \times 4 \times 4$   $q$ -point meshes are used in the interpolation of the phonon calculations. It is ensured the convergence of the phonon frequencies to better than  $1 \text{ cm}^{-1}$ . All the calculations are performed using the ABINIT code [24,25] based on the DFT.

### 3. Results and discussions

#### 3.1. Ground state properties

The filled tetrahedral crystal structures in the  $\alpha$  phase,  $\beta$  phase and  $\gamma$  phase of LiMgN are displayed in Fig. 1, respectively. The equilibrium volume of LiMgN in the  $\alpha$ ,  $\beta$  and  $\gamma$  phase is determined by calculating the total energy as a function of volume as shown in Fig. 2. It is noted that the  $\alpha$  phase is the most stable state for the ZB structure. The equilibrium structural parameters are obtained by fitting the energy–volume curves to the Murnaghan's equation of state [26]. The obtained equilibrium lattice constant  $a_0$ , bulk modulus  $B_0$ , and its pressure derivation  $B'$  are presented in Table 1, together with the available experimental and other theoretical results. Our calculated lattice constant  $a_0$  is slightly larger than the experimental value by 0.36%. The rest of this paper will only focus on the  $\alpha$  phase of the ZB structure LiMgN due to the fact that the equilibrium total energy per formula unit of the  $\alpha$  phase is much lower than that of the  $\beta$  and  $\gamma$  phase.

#### 3.2. Electronic properties

The calculated electronic band structure and density of state along the high symmetry directions of the Brillouin zones at normal pressure and high pressures of the  $\alpha$  phase LiMgN are plotted in Figs. 3 and 4, respectively. The whole band structure outlines are the same with the previous theoretical results [9,10,27]. It is clear that the valence band maximum is located at  $\Gamma$  point, the conduction band minimum occurs at  $X$  point. The calculated band gaps

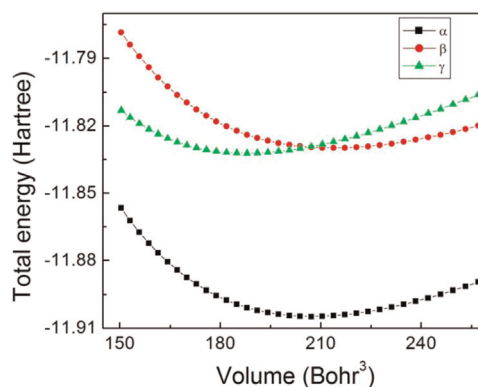


Fig. 2. Total energy per formula unit as a function of volume for the  $\alpha$ ,  $\beta$  and  $\gamma$  phase of the ZB structure LiMgN.

Table 1

Calculated values of equilibrium lattice constant  $a_0$  (Å), bulk modulus  $B_0$  (GPa), and its pressure derivation  $B'$  of LiMgN together with the available experimental and theoretical data.

	This work	Others	Expt.	
$\alpha$ phase	$a_0$	4.973	4.999 [2], 5.009 [9], 4.912 [10], 5.036 [14], 5.010 [28]	4.955 [1]
	$B_0$	108	99 [2], 98 [9], 110 [10]	
	$B'$	3.89	3.99 [9]	
$\beta$ phase	$a_0$	5.022	5.067 [2], 5.079 [9]	
	$B_0$	91	77 [2], 80 [9]	
	$B'$	3.96	3.87 [9]	
$\gamma$ phase	$a_0$	4.810	4.866 [2]	
	$B_0$	103	97 [2]	
	$B'$	4.14		

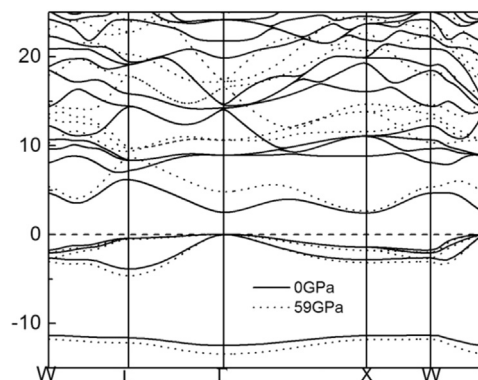


Fig. 3. The electronic band structures for the  $\alpha$  phase of the ZB structure LiMgN at normal and 59 GPa, respectively.

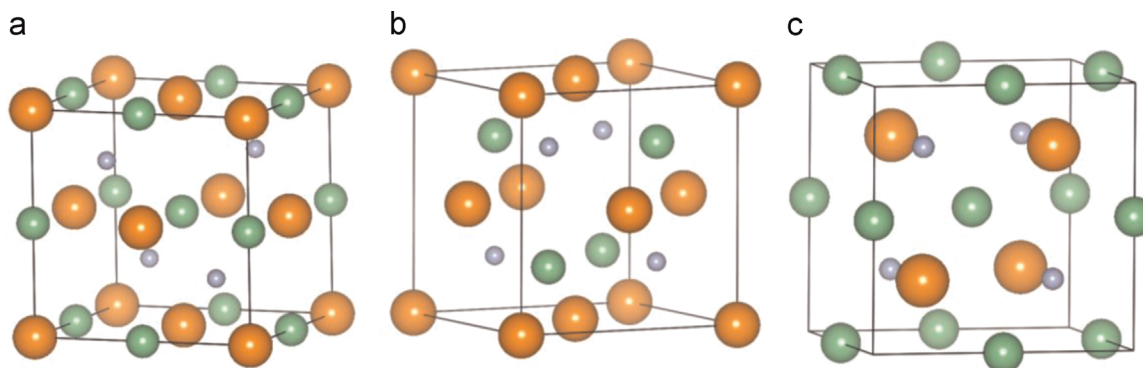


Fig. 1. The filled tetrahedral crystal structure (a)  $\alpha$  phase, (b)  $\beta$  phase, and (c)  $\gamma$  phase of LiMgN. The Mg atoms are the largest balls, the N atoms are the smallest balls, and the Li atoms are the remainder balls.

Download English Version:

<https://daneshyari.com/en/article/1329505>

Download Persian Version:

<https://daneshyari.com/article/1329505>

[Daneshyari.com](https://daneshyari.com)